

V. B. Zheleznyi, A. V. Zagorskii,
S. S. Katsnel'son, A. V. Kudryavtsev,
and A. V. Plekhanov

UDC 533.92;621.384

Researchers have become increasingly interested lately in high-energy processes and in system capable of producing such energies, including those which operate on kinetic principles. Electrodynamical mass accelerators show considerable promise among such kinetic systems. The most widely used of this type are rail-launching electromagnetic accelerators (railguns), largely because of the eminently unsophisticated and simple configuration of the apparatus. Such accelerators are capable of imparting velocities as high as ~5-6 km/sec to projectiles in the gram weight range, but opportunities for achieving higher velocities have been sharply curtailed. It is now apparent that further progress will not be likely without a detailed study of the state of the plasma armature and momentum loss mechanisms in the barrel.

A particularly timely facet of this plan is the development of a physicomathematical model to adequately describe the processes involved in railguns, because patent difficulties are encountered in their experimental investigation, and the experiments themselves are very costly.

However, reliable information can only be obtained by comparing the results of theoretical studies with the experimental. Such a comparison has been made [1, 2] for integral mathematical models of railguns. In the present article we give the results of a series of experiments on the launching of macroscopic bodies (projectiles) and then analyze the results within the framework of integral and quasi-one-dimensional models.

1. A generalized crowbar switch model [3, 4] and a quasi-one-dimensional magnetogasdynamic model [3, 5] are used in the calculations. In the integral model the gasdynamic equations are averaged over the volume of the plasma armature. A closure condition is derived on the basis of the equation of motion of the gas. The resulting system is augmented with an equation expressing Kirchhoff's voltage law for the electrical network. The quasi-one-dimensional model utilizes the one-dimensional magnetogasdynamic equations for the average values of the density, pressure, velocity, and internal energy over the barrel cross section. The electromagnetic variables are determined by solving Maxwell's equations in integral form. Tables of the thermophysical properties of a nonideal plasma [6], calculated by the procedure of [7], are used in both cases. The conductivity values are taken from [8].

As mentioned, any mathematical model of the railgun must correctly mirror the fundamental momentum loss mechanisms in the gun barrel. These mechanisms include wave resistance, friction between the projectile and the barrel wall, turbulent and Hartmann friction, and mass intrusion in the plasma armature by barrel ablation. The influence of the processes are estimated in [3]. We now discuss each of these mechanisms in detail and analyze their influence in comparison with experiment.

Wave Resistance. The projectile is preceded by a powerful shock wave, in whose wake the pressure is given by the expression

$$p_c \approx \rho_0 v^2 \frac{\kappa + 1}{2},$$

where v is the velocity of the projectile, ρ_0 is the undisturbed air density, and κ is the effective adiabatic exponent (specific heat ratio, $\kappa \approx 1.2-1.3$ for air at $v \sim 3-7$ km/sec). Consequently, the drag produced by wave resistance is

$$F_{wr} = S_n \rho_0 v^2 \frac{\kappa + 1}{2}$$

(S_n is the "nose" cross section of the projectile).

Novosibirsk. Translated from *Prikladnaya Mekhanika i Tekhnicheskaya Fizika*, No. 2, pp. 32-36, March-April, 1993. Original article submitted November 22, 1991; revision submitted April 6, 1992.

Projectile-Barrel Wall Friction. The projectile-wall friction coefficient has been determined previously [1, 9]; it decreases with increasing velocity and, beginning with $v \sim 2$ km/sec, remains almost constant and equal to 0.05.

The friction force has the form

$$F_f \approx \frac{\mu(p_n + p_e) S_{lat}}{2 S_n},$$

where μ is the friction coefficient, p_n is the pressure in the plasma armature in the vicinity of the nose of the projectile, and S_{lat} is the lateral surface area of the projectile. It is readily shown that the velocity loss through wall friction is not greater than 2-3% for $S_{lat}/S_n \sim 4$ if the mass of the plasma armature is of the same order as the mass of the projectile itself.

Turbulent Friction. The tangential stress of turbulent friction at the wall is [10]

$$\tau \approx \frac{\lambda}{8} \rho \bar{u}^2$$

(\bar{u} is the average value of the velocity over the barrel cross section, and λ is the dimensionless friction coefficient). Integrating over the volume of the plasma armature, we obtain the estimate for the friction force

$$F_f = \frac{\lambda}{2b} m_{pa} v^2$$

(b is the bore diameter, and m_{pa} is the mass of the plasma armature). For typical railgun characteristics $\lambda \sim 1 \cdot 10^{-2}$, $b \sim (1-2) \cdot 10^{-2}$ m, and $m_{pa} \sim (1-10) \cdot 10^{-3}$ kg and for currents of 500-1000 kA, the influence of turbulent friction becomes appreciable at velocities of 5-6 km/sec.

Ablation of the Barrel Wall. As in [3, 5], we assume that ablation is proportional to the heat flux at the wall:

$$q_{mel} = \frac{1}{A_{el}} Q_{rad}, \quad q_{min} = \frac{1}{A_{in}} Q_{rad}.$$

Here q_{mel} and q_{min} are the mass flow rates from the electrodes and the insulators, A_{el} and A_{in} are their specific energies of vaporization, and Q_{rad} is the radiant heat flux to the wall.

2. We analyze the results of five experiments. The initial data are summarized in Table 1. A free arc was accelerated in the third experiment. The current was measured by Rogowski loops within ~5% error limits, and the position of the projectile in the barrel ($x-t$ diagram) was determined from the readings of induction sensors.

In the fourth experiment the velocity of the projectile in its external trajectory was measured by contact sensors (on a baseline of 3.858-4.368 m from the orifice of the barrel) and had a value ≈ 3.7 km/sec.

Figures 1-5 show the experimentally determined current (x 's), $x-t$ diagrams (circles), and velocity determined by numerical differentiation of the latter (triangles) as functions of the time. The figures are numbered in the order of the experiments. The results of the calculations are represented by solid (quasi-one-dimensional model) and dashed (integral model) curves.

A series of calculations was carried out with the parameters $\lambda = 0.01$, $\mu = 0.05$, $A_{el} = 6 \cdot 10^6$ J/kg, and $A_{in} = 25 \cdot 10^6$ J/kg.

It is evident from Figs. 1-4 that the indicated models give results in good agreement with each other and with the experimental in the values of the current (curve 1) and the position coordinate (curve 2). Estimates show that the discrepancies between the experimental and calculated current curves (Figs. 3-5) around the maximum are attributable to a heating-induced variation in the resistance of the current-carrying armature, which was ignored in the calculations. The difference between the calculated and experimental current oscillograms at the beginning of the process (Figs. 4 and 5) is most likely attributable to error of the ratio U_0/L_M .

More pronounced discrepancies are observed between the velocity values determined from the induction sensor readings and the calculated values (curves 3 in Figs. 1-4) in conjunction with good agreement of the $x-t$ diagrams. This is because a slight error in determining

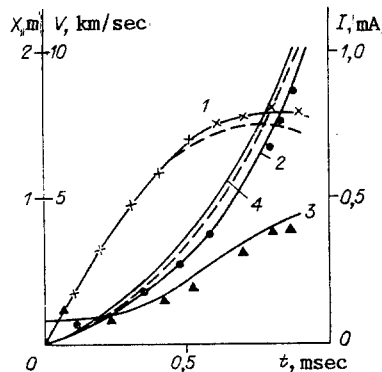


Fig. 1

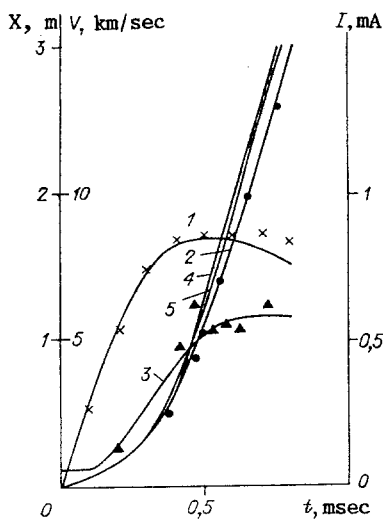


Fig. 2

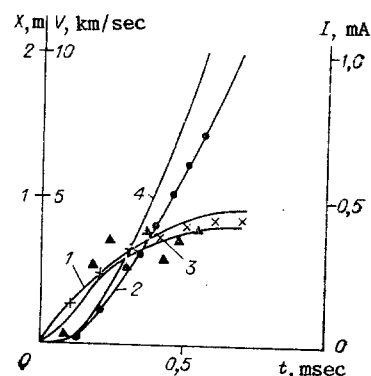


Fig. 3

TABLE 1

Experiment No.	Bank capacitance Φ	Mounting inductance $L_M, \mu\text{H}$	Mounting resistance, $\text{m}\Omega$	Initial voltage U_0, kV	Barrel cross section, mm	Barrel length, m	Projectile mass, g	Initial velocity, m/sec
1	0.2	2.2	0.6	4.3	15×15	2	10	850
2	0.35	1.2	0.47	4.3	15×15	3	3.8	600
3	0.2	2.2	0.6	3.0	20×20	2	—	—
4	0.35	1.2	0.47	4.3	20×20	2	10	400
5	0.35	1.2	0.47	4.3	20×20	2	10	400

the position of the projectile can induce an appreciable velocity error in numerical differentiation. A certain error is also introduced by the transient behavior of the process. A comparison of the calculated and experimental results shows that the error of determination of the position from the inductive sensor readings does not exceed 1-2 bore diameters. This same conclusion has been reported previously in [11].

We have investigated the influence of the various loss mechanisms on the acceleration dynamics, confirming the conclusions of our preliminary analysis: Projectile-wall friction does not have any appreciable influence on the exit velocity. Calculations show that the neglect of this friction factor raises the velocity by 100-150 m/sec. The principal factors responsible for momentum losses are ablation and turbulent friction. Calculations performed with allowance for ablation of the insulators alone give exit velocities 1-1.5 km/sec higher (curves 4 in Figs. 1-4 represent the $x-t$ diagrams of these regimes). Turbulent friction induces velocity losses of the order of 300 m/sec in the fourth experiment and considerably higher (about 1 km/sec) in the acceleration of a lightweight body in a long barrel. Curve 5 in Fig. 2 represents the $x-t$ diagram of the regime with $\lambda = 0$.

It is instructive to compare the results of the fourth and fifth experiments, which were carried out with identical initial data. It is evident from Fig. 5 that, beginning at the time $t \approx 0.6$ msec, acceleration all but ceases, so that the exit velocity is more than 1 km/sec lower than that obtained in the fourth experiment. Such an abrupt change in the launch dynamics can happen as a result of the onset of secondary breakdown in the wake of the plasma armature. In the calculation of this regime, secondary breakdown is simulated by specifying a slender conductive region at a distance of 10 cm from the back of the plasma at a time $t = 0.5$ msec, from which point the dynamics of both discharges is investigated simultaneously. The density of the residual gas in the barrel is assigned values of 10 kg/m^3 and 20 kg/m^3 . Curves 2 and 3 in Fig. 5 show the position of the accelerated projectile in normal operation and with the onset of a shunting arc, respectively. Curves 4 and 5 show the time variation calculations show that the total current does not change in this case, and the $x-t$ diagrams practically coincide, indicating the weak dependence of the process on the residual gas density.

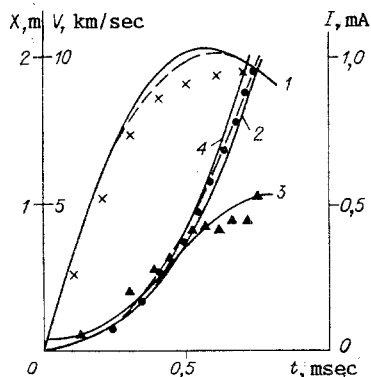


Fig. 4

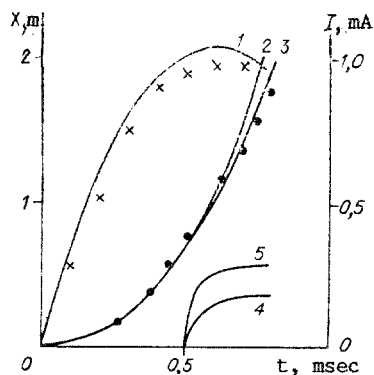


Fig. 5

The reported comparison thus shows that the proposed models taking into account the principal momentum loss mechanisms adequately describe the processes in a railgun and can be used as an effective research tool.

LITERATURE CITED

1. D. A. Weeks, W. F. Weldon, and R. C. Zowarka, "Plasma-armature railgun launcher simulations," *IEEE Trans. Plasma Sci.*, PS-17, No. 3 (1989).
2. R. S. Hawke, W. J. Nellis, G. H. Newman, et al., "Summary of EM launcher experiments performed at LLNL," *IEEE Trans. Magn.*, MAG-22, No. 6 (1986).
3. A. V. Zagorskii and S. S. Katsnel'son, "Mathematical models of the plasma armature in a railgun," in: *Proceedings of the First All-Union Seminar on High-Current Arc Discharge in a Magnetic Field* [in Russian], Institute of Heat Physics, Siberian Branch of the Russian Academy of Sciences (IT SO RAN), Novosibirsk (1990).
4. S. S. Katsnel'son, "Development of a generalized model of a crowbar switch," *Izv. Akad. Nauk SSSR, Sib. Otd., Ser. Tekh. Nauk*, No. 3 (1990).
5. A. V. Zagorskii and S. S. Katsnel'son, "Dynamics of the plasma armature in the barrel of a railgun," *Teplofiz. Vys. Temp.*, 29, No. 3 (1991).
6. G. A. Koval'skaya, *Composition and Thermodynamic Properties of a Copper Plasma: Report* [in Russian], No. 1704, Institute of Theoretical and Applied Mechanics, Siberian Branch of the Russian Academy of Sciences, Novosibirsk (1987).
7. G. A. Koval'skaya, "Composition and thermophysical properties of a nonideal copper plasma," in: *Proceedings of the First All-Union Seminar on High-Current Arc Discharge in a Magnetic Field* [in Russian], Institute of Heat Physics, Siberian Branch of the Russian Academy of Sciences (IT SO RAN), Novosibirsk (1990).
8. N. N. Kalitkin and V. V. Ermakov, *Tables of Conductivities and Electron Thermal Conductivities of Dense Plasmas of 11 Substances*, manuscript deposited at the All-Union Institute of Scientific and Technical Information [in Russian], VINITI Deposit No. 2813-78, Moscow (May 26, 1978).
9. S. Aigner and E. Igenbergs, "Friction and ablation measurements in a round bore railgun," *IEEE Trans. Magn.*, MAG-25, No. 1 (1989).
10. H. Schlichting, *Boundary-Layer Theory*, 6th edn., McGraw-Hill, New York (1968).
11. R. A. Marshall, "Plasma puffing from a railgun armature," *IEEE Trans. Magn.*, MAG-20, No. 2 (1984).